INSTITUTE OF PHYSICS PUBLISHING JOURNAL OF PHYSICS: CONDENSED MATTER

J. Phys.: Condens. Matter **15** (2003) S3557–S3567 PII: S0953-8984(03)66493-3

Phase diagram of hard-core repulsive Yukawa particles with a density-dependent truncation: a simple model for charged colloids

Antti-Pekka Hynninen and Marjolein Dijkstra

Debye Institute, Soft Condensed Matter Physics, Utrecht University, Princetonplein 5, 3584 CC Utrecht, The Netherlands

Received 21 July 2003
Published 20 November 2003
Online at stacks.iop.org/JPhysCM/15/S3557

Abstract

Using computer simulations we study the phase behaviour of hard spheres with repulsive Yukawa interactions and with the repulsion set to zero at distances larger than a density-dependent cut-off distance. Earlier studies based on experiments and computer simulations in colloidal suspensions have shown that the *effective* colloid–colloid pair interaction that takes into account many-body effects resembles closely this truncated Yukawa potential. We present a phase diagram for the truncated Yukawa system by combining Helmholtz free energy calculations and the Kofke integration method. Compared to the non-truncated Yukawa system we observe (i) a radical reduction of the stability of the body centred cubic (BCC) phase, (ii) a wider fluid region due to instability of the face centred cubic (FCC) phase and due to a re-entrant fluid phase and (iii) hardly any shift of the (FCC) melting line when compared with the (BCC) melting line for the full Yukawa potential for sufficiently high salt concentrations, i.e. truncation of the potential does not affect the location of the solid–fluid line but replaces only the BCC phase with the FCC at the melting line. We compare our results with earlier results on the truncated Yukawa potential and with results from simulations where the full many-body Poisson–Boltzmann problem is solved.

(Some figures in this article are in colour only in the electronic version)

1. Introduction

Charge-stabilized colloidal suspensions consist of spherical or anisotropic mesoscopic colloidal particles suspended in a polar solvent with co- and counterions. The standard way to describe the effective one-component colloid–colloid interactions is to use the so-called DLVO theory by Derjaguin, Landau, Verwey and Overbeek [1]. The DLVO theory predicts that, at large separations, the effective-pair interaction between two isolated charged colloidal spheres consists of a hard-core repulsion due to the finite size of the colloids and Yukawa

(screened Coulomb) repulsion with the screening length given by the Debye length κ^{-1} of the electrolyte. The screening length κ^{-1} defines the thickness of the double layer of opposite charge surrounding each colloid. One speaks of a high-salt (low-salt) regime when the double layer around the colloid is concentrated (expanded).

In the regime of high-salt and/or low colloid volume fraction, where there is little overlap of more than two double layers, pairwise additivity is often assumed and the effective colloidal interactions are well described by the hard-core repulsive Yukawa model. However, in the opposite limit of low-salt and (relatively) high colloid volume fraction, the double layers of more than two colloids overlap considerably and there is no guarantee that the assumption of pairwise additivity should work. Instead, the total potential energy of the system is expected to be a sum of many-body (pair, triplet and so on) potentials of the colloids. By now it has been established both experimentally [2] and by computer simulations [3, 4] that these many-body interactions between the colloids do exist and that they manifest themselves as an enhanced decay in the effective colloid pair potential at distances larger than the typical pair separation. Qualitatively this effect can be understood as follows. For a pair of colloids at distances greater than the typical pair separation (at that density ρ), it is likely that there is a third particle between the pair. The effect of the third particle is to screen the repulsion between the pair of colloids, as shown by explicit numerical calculations [4]. The simplest way to incorporate this many-body screening into the colloid pair potential is to state that, after a certain distance, the colloids do not feel each other anymore and therefore the pair force is set to zero [3]. The distance at which the potential is truncated, the so-called cut-off distance, depends on the average separation of colloids, i.e. it is proportional to $\rho^{-1/3}$. This takes us to a simple model for the effective colloid pair potential which has the usual hard-core Yukawa form at distances smaller than the cut-off distance but is set to zero at colloid separations exceeding the cut-off distance. We use this so-called truncated hard-core Yukawa interaction as our effective colloid pair potential and we study the resulting phase behaviour.

The motivation for our study is to find out what are the implications of the cut-off for the phase behaviour of Yukawa particles. In previous works on the phase diagram of the truncated Yukawa system, Dobnikar *et al* [3] used the Lindemann criterion [5] to estimate the solid–liquid phase boundaries. This method, however, is, for example, not suited for studying the relative stability of body centred cubic (BCC) and face centred cubic (FCC) crystal structures. Therefore, we were motivated to calculate the 'exact' phase behaviour of a truncated Yukawa system using a combination of Helmholtz free energy calculations and Kofke integration. Our findings are in agreement with the results of Dobnikar *et al* [3] where it was found that the truncation promotes the fluid phase, i.e. parts of the phase diagram that show a stable crystal phase (BCC or FCC) for the full Yukawa potential are now replaced by the fluid when the potential is truncated. This observation is also supported by Brownian dynamics (BD) simulations where the Poisson–Boltzmann (PB) equation is solved numerically 'on the fly' for each colloid configuration during the BD simulation, i.e. it includes all the effective many-body interactions [3]. These PB–BD simulations are regarded here as the ones that have the correct effective many-body interactions and thus gives the true phase behaviour, while the truncated Yukawa model tries to explain the results only with an effective density-dependent pair interaction that incorporates some of the many-body interactions. The current study makes the phase diagram of truncated Yukawa particles somewhat more precise: we show that the re-entrance of the fluid phase suggested in [3] does indeed exist. More importantly, we demonstrate the instability of the BCC phase with respect to the FCC phase. Destabilization of the BCC phase was also found recently in a simulation study that investigated the effect of triplet attractions on the phase diagram of charged colloids as a first-order correction to pairwise additivity [6].

This paper is organized as follows. In section 2, we present the model and briefly discuss the methods used to calculate the phase diagram. In section 3, we present the results and make comparisons with the results of Dobnikar *et al* [3]. Finally, in section 4 we draw our conclusions.

2. Model and methods

Our model consists of particles interacting with the pairwise repulsive hard-core Yukawa potential that is truncated at a distance which depends on the average distance between the particles. More specifically, our pair potential is given by

$$\beta u(r) = \begin{cases} \infty, & r < \sigma \\ \beta\epsilon \dfrac{\exp(-\kappa\sigma(r/\sigma - 1))}{r/\sigma}, & \sigma \leqslant r < x\rho^{-1/3} \\ 0, & r \geqslant x\rho^{-1/3}, \end{cases} \tag{1}$$

where $\beta\epsilon$ is the value of the pair potential at contact per $k_{\mathrm{B}}T$, κ is the inverse Debye screening length, σ is the hard-core diameter, ρ is the number density of particles and x is a dimensionless constant. In equation (1) $x\rho^{-1/3}$ is the cut-off distance, where $\rho^{-1/3}$ describes the average distance between particles and x is a prefactor that can be used to tune the cut. For example, in a crystal phase x determines how many nearest-neighbour particles are included before the potential is truncated. The choice $x = 1.5$ considered in the current study gives a potential that is truncated for the FCC between the first and second nearest neighbour and between the second and the third for the BCC. With this value for x, both FCC and BCC have approximately equal numbers of neighbour interactions: 12 for FCC and 14 for BCC.

A subtle difference between our model for the cut potential in equation (1) and the one used by Dobnikar *et al* [3] is that, while we truncate the pair potential, they truncate the force. Our motivation to truncate the potential instead of the force stems from the experiments [2] that suggest truncation in the pair potential. In the case of truncation with a smooth decay to zero, i.e. the one proposed by the experiments [2], truncation of both the force and potential yield the same pair potential. However, in the case of non-smooth truncation, there are two differences between a truncated pair potential and a pair potential obtained by integrating the truncated force (called the force-truncated potential in what follows):

(i) the truncated potential has a step to zero at the cut-off distance while the force-truncated potential does not and
(ii) the truncated potential has a fixed contact value $\beta\epsilon$ while the contact value of the force-truncated potential depends on the density.

While the effect of (i) on the phase diagram is not known and would require further studies, the effect of (ii) was studied and found to be small.

Our goal is to calculate the phase diagram of a system in which the particles interact with (1) for fixed contact value $\beta\epsilon = 81$. The phase diagram consists of stable regions of fluid, BCC and FCC phases that are bounded by coexistence regions between the two phases. Therefore the determination of the phase diagram reduces to the calculation of the coexistence curves. We use a combination of Helmholtz free energy calculations [7] and the so-called Kofke integration method [8] to trace out the coexistence curves. In this method Helmholtz free energy calculations are used to obtain phase coexistence points from which Kofke integration can be started to trace the rest of the coexistence curves. The same method has been applied earlier to study the phase diagram of hard-core Yukawa particles without truncation [9] (see also [10] where a similar method has been used). NPT and NVT Monte Carlo (MC) simulations

needed in the Kofke integration and free energy calculations are carried out in a cubic box with periodic boundary conditions [7]. The number of particles used in the simulations is $N = 256$ for the fluid and the FCC phase, and $N = 250$ for the BCC phase.

The results of Dobnikar *et al* [3] were given in the so-called $(\lambda, \tilde{T})$ representation, a typical way to represent phase diagrams of repulsive point Yukawa particles [11, 12], while our results are given in (packing fraction η, Debye screening length $1/\kappa\sigma$) representation. Therefore, in order to compare our results with those in [3], we need to define a mapping between the two systems. The mapping that we present below is the same as in [9], where it was shown that, for sufficiently high $\beta\epsilon$ of the hard-core repulsive Yukawa potential, the phase boundaries are well described by those of point Yukawa particles by employing this mapping.

In the case of point Yukawa particles the relevant length scale is the characteristic interparticle separation $\rho^{-1/3}$. Once $\rho^{-1/3}$ is chosen as the length scale, the pair potential describing the point Yukawa particles can be written as

$$\beta u(r) = \beta U_0 \frac{\exp(-\lambda r/\rho^{-1/3})}{r/\rho^{-1/3}}, \tag{2}$$

where βU_0 is a constant prefactor and λ is the inverse of the screening length in units of $\rho^{-1/3}$. While the phase space of hard-core Yukawa particles is three-dimensional ($\beta\epsilon$, $\kappa\sigma$ and η), only two independent variables exist in the case of point Yukawa particles; since $\rho^{-1/3}$ is chosen as the length scale, there is no need for a density axis. We are therefore left with a two-dimensional phase space consisting of the prefactor βU_0 and the inverse screening length λ. By setting the two pair potentials in equations (1) and (2) to be equal for $r > \sigma$ (and disregarding the cut-off) results in the two equations given by

$$\begin{aligned} &\kappa = \lambda/\rho^{-1/3} \\ &\mathrm{e}^{\kappa\sigma}\sigma\beta\epsilon = \beta U_0 \rho^{-1/3}. \end{aligned} \tag{3}$$

The first line of equation (3) results from setting the exponential decays of the two pair potentials to be equal and the second from the equality of the prefactors. Using the fact that $\rho^{-1/3} = (6\eta/\pi)^{-1/3}\sigma$, we can rewrite equation (3) as

$$\begin{aligned} &\beta U_0 = \mathrm{e}^{\kappa\sigma}\beta\epsilon(6\eta/\pi)^{1/3} \\ &\lambda = \kappa\sigma(6\eta/\pi)^{-1/3}. \end{aligned} \tag{4}$$

Finally, in order to obtain a phase diagram where the phase boundaries can be more or less represented by straight lines, the 'temperature' axis:

$$\tilde{T} = [\tfrac{2}{3}\lambda^2 \beta U_0 u_{\mathrm{M}}(\lambda)]^{-1}, \tag{5}$$

is used instead of βU_0. In equation (5) u_{M} is the Madelung energy of an FCC crystal (i.e. the potential energy of an ideal crystal) per particle per βU_0 [11, 12]. Equations (4) and (5) can be used to map a phase diagram of hard-core Yukawa particles to a phase diagram of point Yukawa particles, and vice versa.

3. Results

In figure 1 we show the phase diagram of particles whose interactions are described by equation (1) with contact value $\beta\epsilon = 81$ and with $x = 1.5$ in the (packing fraction η, Debye screening length $1/\kappa\sigma$) representation. The full curves in figure 1 give the coexistence curves obtained from the Kofke integration that are started from phase equilibria points marked by the squares. These, and the other phase equilibria points marked by the circles, are calculated using the common tangent construction on free energy data obtained from separate Helmholtz

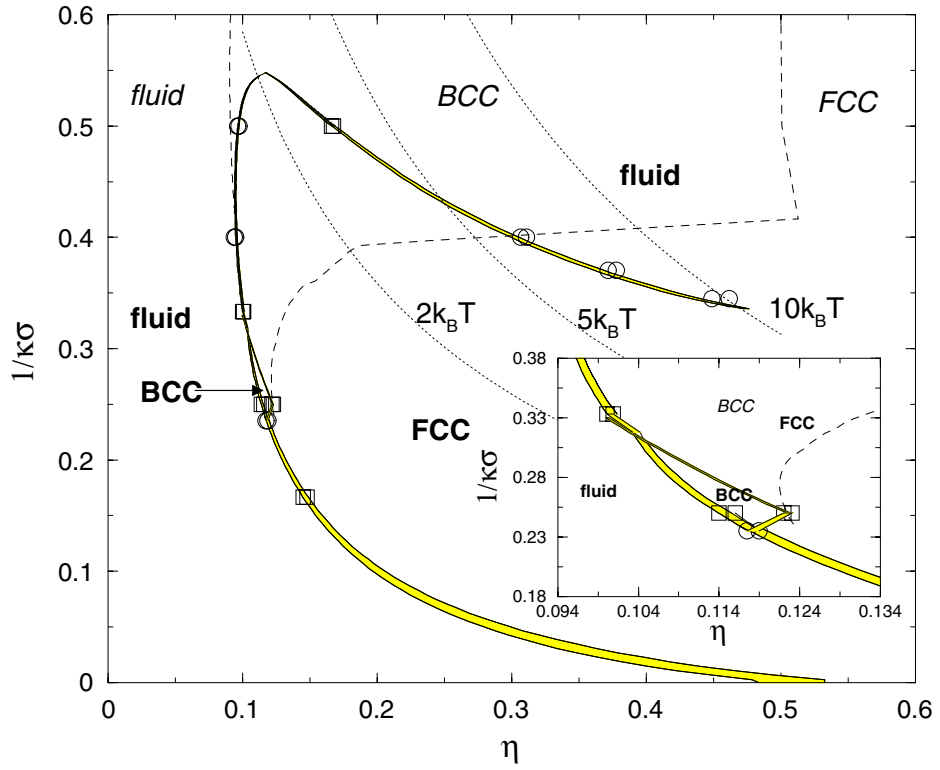

Figure 1. Phase diagram for a system in which the particles interact via a hard-core repulsive Yukawa pair potential (1) with $\beta\epsilon = 81$ and cut-off $x = 1.5$ presented in the (packing fraction η, Debye screening length $1/\kappa\sigma$) plane. The lower part of the diagram ($1/\kappa\sigma = 0$) is the high-salt regime and the upper part ($1/\kappa\sigma = 0.6$) is the low-salt regime. The full curves are coexistence curves obtained by using Kofke integration and the grey areas denote the coexistence regions with horizontal tie lines. The broken curves are the phase boundaries of the hard-core Yukawa particles without truncation from [9] and the dotted curves with labels 2 k_BT, 5 k_BT and 10 k_BT denote the regions where the potential at the cut-off distance is equal to the respective value. The labels 'fluid', 'BCC' and 'FCC' printed in *italic* are for the phase diagram of non-truncated Yukawa particles and the labels printed in **bold** are for the phase diagram of truncated Yukawa particles. The squares mark the starting points for Kofke integration and the circles are check-up points for the coexistence, both of which are obtained using free energy calculations. The inset shows a close-up of the BCC pocket region.

free energy calculations. See table 1 for numerical values of the phase equilibria points. The coexistence regions are shaded, while the tie lines are horizontal. The dotted curves with labels 2 k_BT, 5 k_BT and 10 k_BT denote the regions where the potential at the cut-off distance is equal to the respective value. This means, for example, that at the right-hand side of the curve labelled by 2 k_BT the value of the potential at the cut-off is larger than 2 k_BT. For comparison we plot the phase diagram of the non-truncated Yukawa system obtained from [9] (broken curves). The phases for the non-truncated and truncated Yukawa systems are labelled in *italic* and **bold**, respectively. The inset in figure 1 shows a close-up of the BCC pocket region.

The phase diagram in figure 1 starts from the hard-sphere fluid–FCC coexistence at $1/\kappa\sigma = 0$ ($\kappa\sigma = \infty$). As the softness and range of the interactions increase, i.e. $1/\kappa\sigma$

Table 1. Phase coexistence points of figure 1 (squares and circles) obtained from free energy calculations. $\beta P\sigma^3$ gives the dimensionless pressure and η_1 and η_2 give the packing fractions of the two phases at coexistence. The pressure is only given at coexistence points from which Kofke integration was started (the squares in figure 1).

$1/\kappa\sigma$	$\beta P\sigma^3$	η_1	η_2	Phases
0.167	5.94	0.145	0.148	Fluid–FCC
0.235	—	0.118	0.119	Fluid–FCC
0.250	6.29	0.114	0.116	Fluid–BCC
0.250	7.53	0.122	0.123	BCC–FCC
0.333	7.31	0.100	0.101	Fluid–FCC
0.345	—	0.450	0.460	FCC–fluid
0.370	—	0.372	0.378	FCC–fluid
0.400	—	0.094	0.095	Fluid–FCC
0.400	—	0.307	0.311	FCC–fluid
0.500	—	0.097	0.098	Fluid–FCC
0.500	37.62	0.166	0.169	FCC–fluid

increases, the fluid–FCC coexistence becomes narrower and moves to lower packing fractions until a fluid–BCC–FCC triple point is reached at $1/\kappa\sigma \approx 0.24$. Below the triple point ($1/\kappa\sigma < 0.24$), the truncated and non-truncated potential give basically the same result for the fluid–FCC coexistence curves. The reason for this is that in this regime, where $\kappa\sigma$ is high (and the density is low), the pair potential decreases to be close to zero when the cut-off distance is reached, and therefore the two systems behave in the same manner. Above the triple point ($1/\kappa\sigma > 0.24$), important deviations between the results of the truncated and non-truncated potential emerge: while the system with Yukawa interactions has a large BCC pocket (the region bounded by the broken curves), only a small region of BCC is seen in the truncated Yukawa system. This region is concentrated close to the fluid–BCC–FCC triple point at $1/\kappa\sigma \approx 0.24$. The instability of the BCC phase is due to the short-range nature of the truncated potential: BCC is the stable phase in systems that have soft long-range interactions. This is why we expect that, when the cut is made larger, i.e. x is made smaller, the stability of the BCC phase is reduced even further. Conversely, with a milder cut, i.e. with larger x, more BCC phase is expected to be present. Indeed, preliminary free energy calculations with $x = 1.77$ showed a stable BCC phase at $1/\kappa\sigma = 0.4$. Destabilization of the BCC phase was also found recently in a simulation study that investigated the effect of triplet attractions on the phase diagram of charged colloids as a first-order many-body correction to pairwise additivity [6].

It is also worth mentioning that the fluid–FCC phase boundary above the second triple point follows closely the fluid–BCC phase boundary of the non-truncated Yukawa system. Thus, the sole effect of the truncation on the melting curve at low η is that the BCC phase is replaced by the FCC.

Another effect of the truncation seen in figure 1 is a re-entrance of the fluid phase above $1/\kappa\sigma = 0.35$ at higher η, i.e. one observes a sequence of fluid, FCC and again a fluid phase with increasing colloid volume fraction. Re-entrance is not seen in Yukawa systems [9–12] but has been observed in an earlier study on truncated Yukawa systems [3]. Although not studied here further, we expect that, because of the hard-core interaction, the fluid phase will freeze again to the FCC phase at high enough packing fractions, around $\eta \approx 0.5$. The reason why this re-freezing transition was not studied here is that the description using the truncated potential fails to represent any physically relevant system when the cut becomes too large. From figure 1 we see that at re-freezing the cut would be more than $10\,k_{\mathrm{B}}T$.

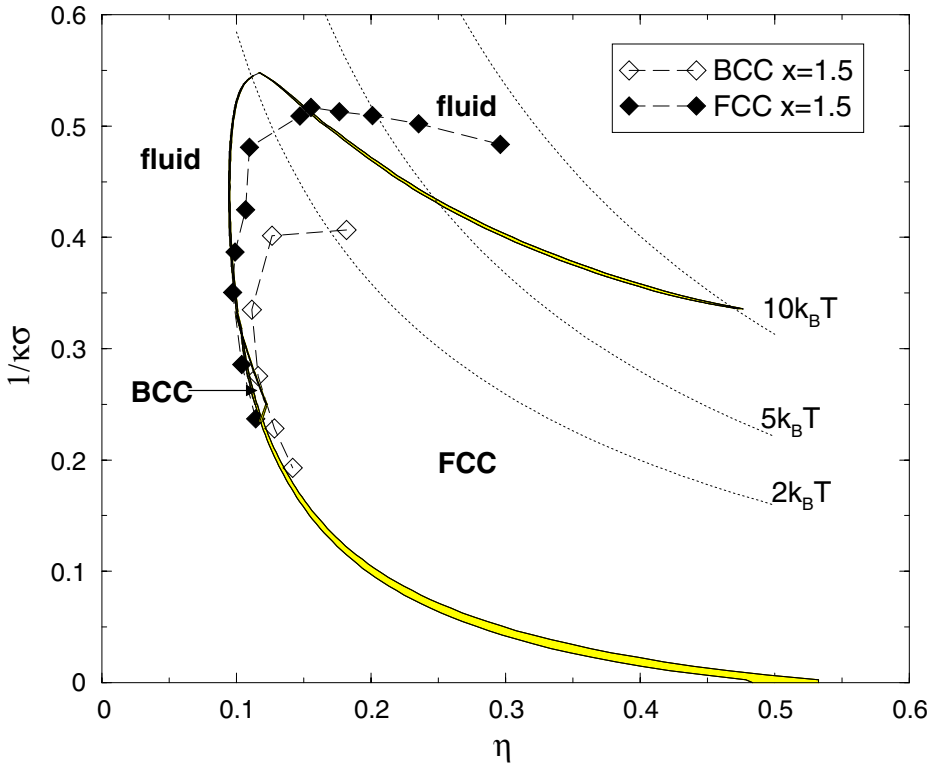

Figure 2. Phase diagram for a system in which the particles interact via a hard-core repulsive Yukawa pair potential (1) with $\beta\epsilon = 81$ and cut-off $x = 1.5$ presented in the (packing fraction η, Debye screening length $1/\kappa\sigma$) plane. The low part of the diagram ($1/\kappa\sigma = 0$) is the high-salt regime and the upper part ($1/\kappa\sigma = 0.6$) is the low-salt regime. The full curves are coexistence curves obtained by using Kofke integration and the grey areas denote the coexistence regions with horizontal tie lines. The filled and open diamonds connected with long-dashed curves are, respectively, the FCC and the BCC melting curves for a truncated point Yukawa system with $x = 1.5$ from [3]. The dotted curves with labels 2 k_BT, 5 k_BT and 10 k_BT denote the regions where the potential at the cut-off distance is equal to the respective value.

In the low-salt regime in figure 1, from around $1/\kappa\sigma = 0.4$ upwards, one sees that the fluid–solid phase boundaries with and without truncation deviate from each other (the difference between the broken and the full curves); a system with truncation has more fluid phase. Moreover, at $1/\kappa\sigma \approx 0.55$ the fluid–FCC and the re-entrant FCC–fluid phase coexistence curves join, implying that above this point only the fluid phase is stable.

In figure 2 we compare our results with the truncated-point Yukawa system of Dobnikar *et al* [3]: the filled and open diamonds connected with long-dashed curves mark the FCC and BCC melting curves for a truncated-point Yukawa system with $x = 1.5$. Before analysing figure 2 further, we wish to make a few remarks on the Lindemann criterion, which was employed in [3]. The Lindemann criterion states that, at the melting curve, the root mean square displacements of the particles about their equilibrium positions in the crystal phase is a universal fraction of the interparticle distance a, often taken to be 0.19 [5]. The solid phase should always be the stable phase immediately at the melting curve. A simulation started from a *metastable* solid phase melts at lower temperatures or higher packing fractions than

the stable solid phase [11]. Figure 2 shows that the truncated Yukawa BCC melting curve of [3] is at a higher packing fraction than the FCC melting curve for all $1/\kappa\sigma$, indicating that the BCC phase is always metastable with respect to the FCC phase at the solid–fluid phase boundary. The agreement of the FCC melting curve with our fluid–FCC phase coexistence curve is reasonable but gets worse with increasing $1/\kappa\sigma$. In particular the prediction for the re-entrant FCC–fluid phase boundary clearly deviates from our result. The method in [3] based on the Lindemann criterion was not accurate enough to find the tiny pocket of stable BCC phase at the melting curve. It is tempting to relate the BCC melting curve to the BCC–FCC phase boundary as was done, although very implicitly, in [3]. However, to our knowledge, it has never been tested that a universal behaviour of the root mean square displacement holds at the solid–solid phase boundaries similar to that at the melting curve, as stated by the Lindemann criterion. Comparing the BCC melting curve obtained from the Lindemann criterion with our 'exact' phase diagram, we indeed see that this curve cannot be associated with any of our phase boundaries.

In figure 3 we show results from figure 2 combined with the PB–BD results of Dobnikar *et al* [3] in the $(\lambda, \tilde{T})$ representation. The open circles and full squares denote the melting points obtained from the PB–BD simulations while the (thin) full curves give our results. The thick full curves show the fluid–solid and BCC–FCC phase boundaries of point Yukawa particles without truncation [12]. Please note that, according to these non-truncated point Yukawa results, the triangle formed by the thick curves has a stable BCC phase. From figure 3 we find that in our results the BCC phase is replaced by FCC, while the PB–BD results indicate that the BCC phase gets substituted by fluid. The only agreement between our results and the PB–BD results is that both show more fluid phase than what is found when no truncation is used. Because of the lack of data, it cannot be said if the re-entrance, seen in the truncated Yukawa results, would appear in PB–BD simulations. Keeping in mind that the FCC melting curve is obtained from the Lindemann criterion for fluid–solid transitions, it is rather surprising that it follows so accurately the BCC–FCC curve of the full Yukawa system. However, as already mentioned before and shown to be incorrect for the truncated Yukawa system, we should be very cautious in using the Lindemann criterion to predict any phase boundaries other than the fluid–solid one.

Finally we would like to discuss some problems that arise when comparing the many-body PB–BD simulation results with results obtained using a pairwise Yukawa potential. The PB–BD simulation melting points of [3] were determined for several values of κ^{-1} by varying the charge Z at a *single* packing fraction $\eta = 0.03$. Once the melting point Z and κ^{-1} were known, the effective charge Z_{eff} and screening length κ_{eff}^{-1} were estimated. These effective values of Z and κ^{-1} are needed in order to make comparisons with systems interacting with a pairwise Yukawa potential. As long as the hard core does not play a role, and this is to be expected at $\eta = 0.03$, it is then possible to plot the results in the $(\lambda, \tilde{T})$ representation using the effective charge Z_{eff} and screening length κ_{eff}^{-1}, as was done in [3]. In order to replot our truncated Yukawa results from figure 2 in the $(\lambda, \tilde{T})$ plane, we employ the mapping that was presented in section 2 and which is only valid when the hard core does not play an important role. The effect of the hard core on the phase behaviour of the Yukawa system was studied earlier [9] and it was found for $\beta\epsilon = 81$ that only at high packing fractions, around $\eta = 0.5$, does the hard-core interaction lead to deviations in the phase behaviour. In figure 2 only the very end of the re-entrant FCC–fluid phase coexistence curve reaches such high packing fractions that one might expect deviations from the point Yukawa system. Therefore, our results can be plotted in the $(\lambda, \tilde{T})$ plane. If the PB–BD simulation would be repeated at a different volume fraction than η, possibly a different phase diagram in the $(\lambda, \tilde{T})$ plane would be obtained. This is because the effective charge Z_{eff} and screening length κ_{eff}^{-1} depend on η. However, the

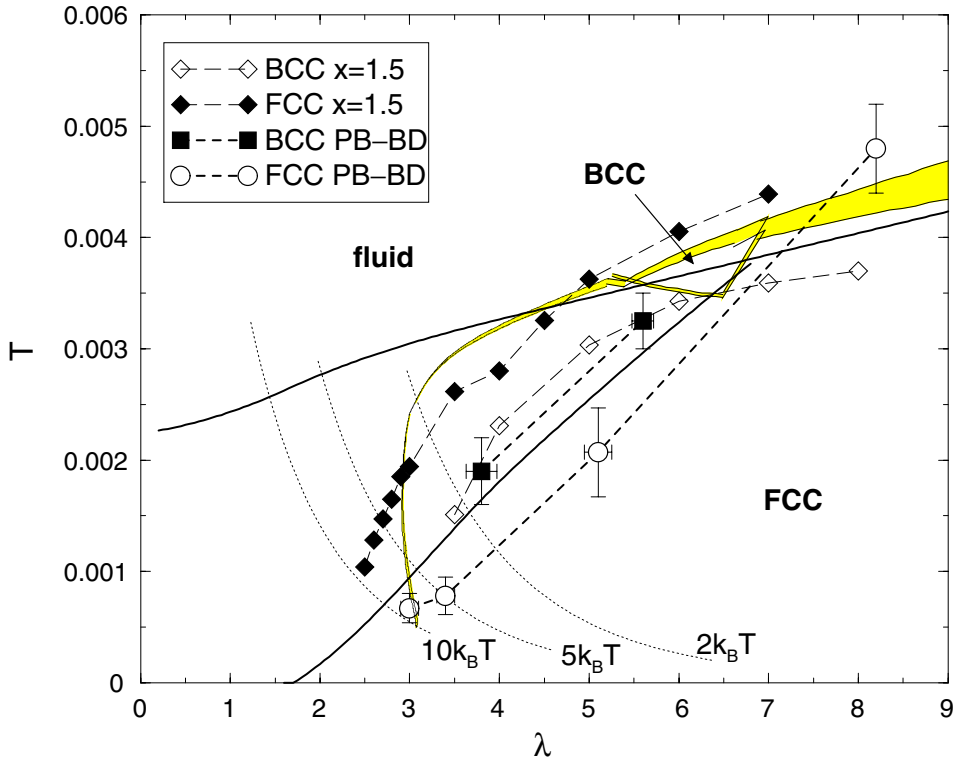

Figure 3. Phase diagram in the $(\lambda, \tilde{T})$ representation. The thick full curves are the phase boundaries for point Yukawa particles obtained by Hamaguchi *et al* [12] and the (thin) full curves are the phase boundaries for a system of truncated hard-core Yukawa particles with $\beta\epsilon = 81$ and with cut-off $x = 1.5$. The hard-core Yukawa results are plotted using the mapping given in [9]. The filled and open diamonds connected with long-dashed curves are, respectively, the FCC and the BCC melting curves for $x = 1.5$ from [3]. The circles and the filled squares with error bars give the melting points of [3] for FCC and BCC phases, respectively, obtained from the PB–BD simulations where the full PB equation is solved giving the 'exact' effective many-body interaction for the colloids. The dotted curves with labels 2 k_BT, 5 k_BT and 10 k_BT denote the regions where the potential at the cut-off distance is equal to the respective value.

pairwise Yukawa results, both ours and those from [3], can still be compared with the PB–BD results in the $(\lambda, \tilde{T})$ plane.

4. Conclusions

The phase diagram of a system where the particles interact with the truncated hard-core repulsive Yukawa potential of equation (1) was studied with contact value $\beta\epsilon = 81$ and cut-prefactor $x = 1.5$. We observed:

(i) a radical reduction of the stability of the BCC phase with respect to the FCC phase,
(ii) more fluid phase due to instability of the FCC phase and due to a re-entrant fluid phase, and
(iii) for sufficiently high salt concentrations, hardly any shift of the FCC melting curve when compared with the BCC melting curve for the full Yukawa potential.

That is, truncation of the potential does not affect the location of the solid–fluid line, but only replaces the BCC phase with FCC at the melting curve. Of these observations (ii) has already been confirmed by Dobnikar *et al* [3] in the truncated-point Yukawa system, However, whether observations (i) and (iii) are supported by the earlier study cannot be answered since the Lindemann criterion used in [3] is not suited to resolve the relative stability of the BCC and FCC phases. Finally, we like to stress that (i), the instability of the BCC phase, was also found recently in our simulation study where the effect of triplet attractions on the phase diagram of charged colloids was investigated [6]. The effect of many-body interactions on the phase behaviour is a destabilization of the BCC phase, which should be observable in experiments.

Only one value of the cut $x = 1.5$ was used in this study. It is natural to expect that, if x is made larger, all three effects (i), (ii) and (iii) mentioned earlier will become less pronounced and finally vanish at $x = \infty$. Conversely, with smaller x, we expect that the three effects become more pronounced.

The only agreement with the full Poisson–Boltzmann Brownian dynamics (PB–BD) simulation results is the increase in the fluid phase. In order to obtain a more quantitative comparison, a different cut prefactor x for fluid, BCC and FCC phases should probably be used. Also, in order to have a pair potential that agrees more with the real effective-pair potential, instead of truncating the potential, a smooth decay to zero should be made. As a preliminary result we have seen that adding a smooth truncation alters the phase behaviour of the system. For example, it is natural to expect that the BCC phase becomes more stable when introducing a smooth decay. However, playing with the cut and adding a smooth truncation increases the number of parameters considerably, and the real problem is how to choose these parameters realistically. One way to obtain them would be to perform PB–BD simulations and extract the parameters by fitting to an effective pair potential. Finally, it is worth noting that, since we are using a very simplified model to incorporate some of the many-body effects, one might not even expect good agreement with the PB–BD results and, thus, a direct comparison between both approaches is difficult. We also like to mention that it would be highly desirable to have more results on the phase behaviour from the full PB–BD simulations in order to be able to make more definite conclusions about the many-body interactions, e.g. when are they important and what is the effect of them on the phase behaviour and structure of the colloidal suspension. Still, we think that our work captures the general features of the phase diagram when a Yukawa potential with (some kind of) truncation is used.

Acknowledgments

The authors would like to thank H H von Grünberg and J Dobnikar for many useful discussions and for providing the numerical data from [3]. We also acknowledge René van Roij and P Royall for stimulating discussions. This work is part of the research program of the 'Stichting voor Fundamenteel Onderzoek der Materie (FOM)', which is financially supported by the 'Nederlandse Organisatie voor Wetenschappelijk Onderzoek (NWO)'. We thank the Dutch National Computer Facilities foundation for access to the SGI Origin3800. The High Performance Computing group of Utrecht University is gratefully acknowledged for ample computer time.

References

[1] Derjaguin B and Landau L 1941 *Acta Phys. Chim. URSS* **14** 633
Verwey E J W and Overbeek J Th G 1948 *Theory of the Stability of Lyotropic Colloids* (Amsterdam: Elsevier)

[2] Brunner M, Bechinger C, Strepp C W, Lobaskin V and von Grünberg H H 2002 *Europhys. Lett.* **58** 926
Klein R, von Grünberg H H, Bechinger C, Brunner M and Lobaskin V 2002 *J. Phys.: Condens. Matter* **14** 7631
[3] Dobnikar J, Chen Y, Rzehak R and von Grünberg H H 2003 *J. Chem. Phys.* **119** 4971
Dobnikar J, Rzehak R and von Grünberg H H 2003 *Europhys. Lett.* **61** 695
Dobnikar J, Chen Y, Rzehak R and von Grünberg H H 2003 *J. Phys.: Condens. Matter* **15** S263
[4] Russ C, von Grünberg H H, Dijkstra M and van Roij R 2002 *Phys. Rev.* E **66** 011402
[5] Lindemann F A 1910 *Z. Phys.* **11** 609
[6] Hynninen A-P, Dijkstra M and van Roij R 2003 *J. Phys.: Condens. Matter* **15**
[7] Frenkel D and Smit B 2002 *Understanding Molecular Simulations* 2nd edn (London: Academic)
[8] Kofke D A 1993 *Mol. Phys.* **78** 1331
Kofke D A 1993 *J. Chem. Phys.* **98** 4149
[9] Hynninen A-P and Dijkstra M 2003 *Phys. Rev.* E **68** 021407
[10] Meijer E J and El Azhar F 1997 *J. Chem. Phys.* **106** 4678
El Azhar F, Baus M, Ryckaert J-P and Meijer E J 2000 *J. Chem. Phys.* **112** 5121
[11] Robbins M O, Kremer K and Grest G S 1988 *J. Chem. Phys.* **88** 3286
[12] Hamaguchi S, Farouki R T and Dubin D H E 1997 *Phys. Rev.* E **56** 4671